

Sign change of Hall coefficients for amorphous $\text{Ni}_{0.80-x}\text{Cr}_x\text{P}_{0.20}$ alloys

K. Rhie and D. G. Naugle

Department of Physics, Texas A&M University, College Station, Texas 77843-4242

Beom-hoan O and J. T. Markert

Department of Physics, University of Texas at Austin, Austin, Texas 78712

(Received 18 October 1993; revised manuscript received 11 January 1994)

The magnetic susceptibilities, resistivities, and Hall coefficients of amorphous $\text{Ni}_{0.80-x}\text{Cr}_x\text{P}_{0.20}$ ($0.00 \leq x \leq 0.40$) alloys are reported. A sign change with temperature of the Hall coefficient for a single paramagnetic amorphous alloy that correlates with the temperature-dependent valence susceptibility has been observed ($x=0.20$), indicating that an extraordinary contribution to R_H is responsible for the positive Hall effect in these paramagnetic alloys. Also, an unexplained relatively large contribution to R_H that is linear in T has been observed in some of these alloys. A gradual change in magnetic properties with composition from large cluster-dominant phase to Kondo-impurity phase has been observed.

I. INTRODUCTION

The widespread occurrence of a positive Hall coefficient (R_H) for amorphous non-magnetic transition-metal (TM) alloys¹ as compared to the negative almost free-electron value for almost all simple amorphous alloys² has been a puzzle in electron transport in glassy metals. Since the first observation of positive values of R_H for nonmagnetic amorphous transition-metal alloys, La-Al and La-Ga,^{3,4} similar observations followed in early TM (ETM)-late TM (LTM) and ETM-simple metal (SM) alloys. For some time, the positive R_H for Cu-Zr and similar alloys was explained in terms of a negative group velocity of conduction electrons due to s - d band hybridization.⁵⁻⁷ However, the side-jump effect, an extraordinary contribution to R_H , which originates from the spin-orbit interaction, has recently been considered as an important effect in these alloys.

Trudeau *et al.*⁸ suggested that the side-jump effect, an asymmetric scattering of conduction electrons due to the spin-orbit interaction,^{9,10} is responsible for the temperature-dependent positive R_H of paramagnetic $\text{Zr}_{1-x}\text{Fe}_x$ alloys near the ferromagnetic transition regime. The side-jump contribution to the Hall resistivity is given as⁸⁻¹¹

$$R_H = R_H^0 + R_H^{\text{SJ}} \chi_v, \quad (1.1)$$

where R_H is the measured Hall coefficient, R_H^0 is the Lorentz term, and $R_H^{\text{SJ}} \chi_v$ is the extraordinary contribution by the side-jump effect. The side-jump effect term can be summarized as

$$\rho_H^{\text{SJ}} \chi_v = \sum_i \frac{2\rho^2 N_i q_i^2}{\hbar} \lambda_{\text{SO}}^{\text{SJ}} \langle S_z \rangle \quad (1.2)$$

or

$$\chi_v R_H^{\text{SJ}} = \frac{2e^2}{\mu_0 \hbar g \mu_B} \rho^2 \lambda_{\text{SO}}^{\text{SJ}} \chi_v$$

with

$$\lambda_{\text{SO}}^{\text{SJ}} = \sum_n \frac{|\langle n | \mathbf{L} | 0 \rangle|^2}{\epsilon_n - \epsilon_F} l^2 A_{\text{SO}}, \quad (1.3)$$

where i denotes carrier type, q_i denotes the charge of i -type carriers, $\lambda_{\text{SO}}^{\text{SJ}}$ denotes the effective spin-orbit parameter, A_{SO} is the atomic spin-orbit parameter, l is the overlap integral, and l is the distance between the scatterers. If two kinds of transition metals of ETM and LTM work as spin-orbit scatterers, Eq. (1.3) can be written as¹²

$$\lambda_{\text{SO}}^{\text{SJ}} = \{ l^2 A_{\text{SO}} \Sigma \}_{\text{ETM}} + \{ l^2 A_{\text{SO}} \Sigma \}_{\text{LTM}} \quad (1.4)$$

and

$$\Sigma_i = \int_{-\infty}^{\infty} \frac{|\langle \epsilon | \mathbf{L} | 0 \rangle|^2}{\epsilon} g_i(\epsilon) d\epsilon,$$

where $i = \text{ETM, LTM}$ and $g_i(\epsilon)$ is the density of states. A theoretical band calculation could provide a prediction of the variation of $\lambda_{\text{SO}}^{\text{SJ}}$ for comparison with experiments. The $\lambda_{\text{SO}}^{\text{SJ}}$ of 3- d and 4- d electrons is about 10^4 times larger than that of free electrons.^{10,12}

Rhie, Naugle, and Bhatnagar reported that the values of R_H for $(\text{Zr}_{0.64}\text{Ni}_{0.36})_{1-x}\text{Al}_x$ (Ref. 13) and $(\text{Zr}_{0.50}\text{Ni}_{0.50})_{1-x}\text{Al}_x$ (Ref. 14) alloys increase with x , which is difficult to understand in terms of the s - d band hybridization model. They argued that the side-jump effect could explain the unusual variation of R_H in pseudobinary Zr-based amorphous alloys produced by varying the simple metal doping. More recently they have shown that the variety of behavior of R_H observed for Zr-based binary alloys could be explained by the variation of $\lambda_{\text{SO}}^{\text{SJ}}$ due to the location of the Fermi level for different alloys.^{12,15}

The ferromagnetic $\text{Ni}_{1-x}\text{P}_x$ alloy system ($x \leq 0.18$) provides a good example of the side-jump effect in ferromagnetic alloys.^{10,11} The Fermi level of $\text{Ni}_{1-x}\text{P}_x$ lies in the upper half of the Ni d band, and the binding energy decreases as the Ni content increases. The 0.6 holes of

the pure Ni d band is well known; such holes are responsible for the negative λ_{SO}^{SJ} and R_H for pure Ni and $Ni_{1-x}P_x$ alloys. Photoemission experiments indicate that there are two broad, well-defined d bands in amorphous early transition-metal-late transition-metal alloys.¹⁶ In these alloys the center of the late transition-metal d band lies below the Fermi energy while that of the early transition-metal d band lies above the Fermi energy. This feature of the electronic structure has been explained qualitatively in terms of renormalized atom calculations,¹⁷ which in the case of Zr-based alloys leads to a split band picture. The predicted density of states is in reasonable agreement with the available Zr- X photoemission data and explains the observed relationship between the superconducting transition temperatures of further Zr- X alloys. In this model for the electronic structure the negative λ_{SO}^{SJ} should become positive when sufficient Ni is substituted with Cr, as the unfilled Ni d band fills up and the Fermi level lies in the lower half of the higher-energy Cr d band.

This experiment was designed to test two points. First, R_H of the $Ni_{0.80-x}Cr_xP_{0.20}$ alloys should be temperature dependent, because the side-jump effect or anomalous Hall resistivity is proportional to the spin polarization of the conduction electrons. The magnetic susceptibility of $Ni_{0.80}P_{0.20}$ at high field is reported to be temperature dependent so that the value at 10 K is about three times larger than the room-temperature value.¹⁸⁻²¹ Second, as x increases, a change of sign of R_H from negative to positive as the anomalous side-jump contribution changes sign with additive Cr should be observed, provided that the anomalous term overcomes the ordinary term.

II. EXPERIMENTAL

The 99.6% pure Ni_2P , and CrP, and 99.99% pure Ni and Cr were melted in an Ar atmosphere and melt quenched by an ordinary single roller method to produce 20–30- μ m-thick, 2–3-mm-wide ribbon samples. The magnetization was measured using a commercial superconducting quantum interference device magnetometer. The high-field magnetic susceptibility was measured at 1 T, as the system cooled from 300 K to 10 K. The zero-field-cooled and field-cooled methods were used at 5×10^{-4} T to observe the superparamagnetic cluster blocking or spin-glass transition. The low-field susceptibility was obtained from the field-cooled data. The absolute error of the susceptibility measurement is less than 1%. The five-probe method was used for the Hall-effect measurement. The samples were partially cut along the edges of the ribbon at three locations to make ears, and the wires for Hall voltage were spot welded at the ends of these ears. This method enables the electric currents to avoid the locally crystallized spot welded area which might contain a ferromagnetic phase and give a nonlinear Hall resistivity.²² Contact instabilities, however, limited Hall-effect measurements for $x > 0.20$ to room-temperature values. A magnetic field up to 5 T was applied normal to the ribbons to measure R_H at fixed temperatures. Electron microprobe analysis wavelength dispersion spectroscopy was used to measure the compo-

sitions of ribbons. Absolute accuracy is better than 1 at. %, and the relative accuracy is better than 0.5 at. %. Trace elements of Fe and Co are also measured with a low detection limit of 200 ppm.

III. RESULTS AND DISCUSSION

The total magnetic susceptibility (χ_T) at high field can be written as

$$\chi_T = M/H = \sigma(H, T)/H + \chi(T)$$

$$\text{with } \chi(T) = \frac{C}{T + \theta} + \chi_0, \quad (3.1)$$

where $\sigma(T)$, which is dominant at $x = 0.00$ and 0.02, but is negligible for $x \geq 0.10$, is the temperature-dependent net saturation moment of ferromagnetic clusters in a M vs H plot, and $\chi(T)$ is the high-field slope of the magnetization (M vs H) curve, which includes a temperature-dependent Curie term and a temperature-independent χ_0 (Pauli paramagnetic, diamagnetic, and Van Vleck) contribution. It also includes the superparamagnetic clusters of smaller magnetic moment that are not saturated yet. A Curie-Weiss fit is just a conventional, but not a rigorous analysis. Rhie *et al.*²³ have suggested that a power law [$\chi(T) = C/T^p + \chi_0$] provides a better fit of $M(T)$ for paramagnetic amorphous metallic alloys near the ferromagnetic phase with negligible superparamagnetic clusters of the ferromagnetic phase.

Figure 1 shows the high-field susceptibility $\chi(T)$ for $x = 0.00$ and χ_T at 1 T for $0.25 \geq x > 0.00$. Our measurement of $\chi(T)$ for $x = 0.00$ is less temperature dependent, i.e., can be fit with a smaller Curie constant (38.91 μ emu/mol K) than that reported by Bugstaller *et al.*²¹ (250 μ emu/mol K), because our measurements for $x = 0.00$ were at higher magnetic field (2–4 T) compared to (0.2–1 T in their experiment), so that in this figure the contribution of clusters to $\chi(T)$ is more efficiently eliminated by saturation. The value of χ_{Pauli} (70 μ emu/mol), which is calculated from χ_0 , obtained in the Curie-Weiss fit, however, is comparable to their values (84 μ emu/mol). The Curie constant C is highest at $x = 0.05$, and decreases with x , but $\chi(T)$ at the room temperature increases with x , indicating the increase of the density of states at the Fermi level with increasing Cr concentration. This implies that the Cr d -band states start to dominate at the Fermi level with the addition of small amounts of Cr to $Ni_{0.80}P_{0.20}$.

The total magnetization for $x = 0.00$ (first inset of Fig. 1) is dominated by $\sigma(T)$ of ferromagnetic clusters. Zero-field-cooled and field-cooled magnetization curves split at 300 K, the highest temperature, indicating that the blocking of these clusters has occurred already at 300 K. This means that these ferromagnetic clusters are so big that they are insensitive to the temperature change. $\sigma(T)$ for $x = 0.02$, which is larger than that for $x = 0.00$ at low temperature, decreases rapidly and approaches zero at room temperature. Such a strong temperature-dependent $\sigma(T)$ was also observed in $Fe_{0.33}Zr_{0.67}$ alloys.²³ The authors concluded that the superparamagnetic clusters above the blocking temperature are responsible. We

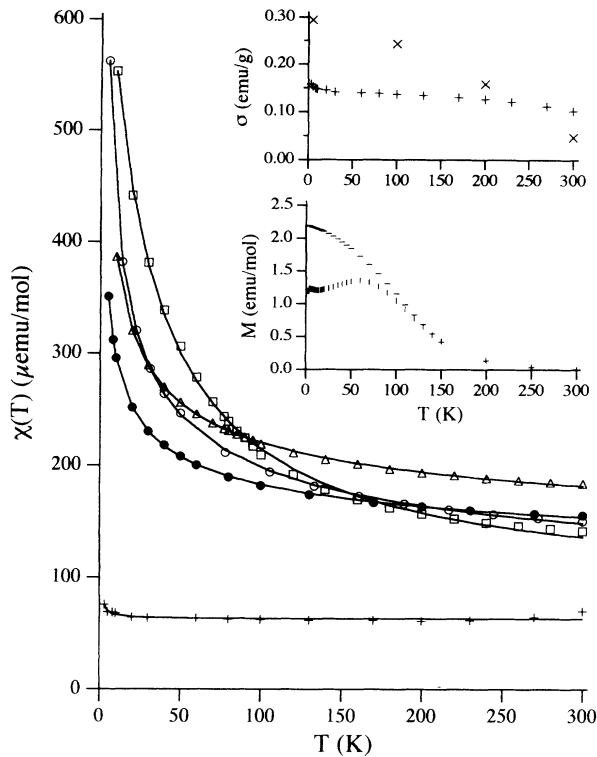


FIG. 1. χ_T vs T of $\text{Ni}_{0.80-x}\text{Cr}_x\text{P}_{0.20}$ alloys at high field. $\chi(T)$ ($=\partial M/\partial H$ at 2 T) of $x=0.00$ (+) and total magnetic susceptibility χ_T ($=M/H$ at 1 T) for $x=0.05$ (□); $x=0.10$ (○); $x=0.20$ (△); and $x=0.25$ (●). We assumed $\sigma(T)=0$ for $x \geq 0.05$ for this fit. The lines are Curie-Weiss fits for each alloy. The first inset shows $\sigma(T)$ for $x=0.00$ (+) and $x=0.02$ (×). The second inset shows the split of zero-field-cooled (—) and field-cooled (|) magnetization (5×10^{-4} T) for $x=0.02$.

expect that the ferromagnetic phase for $x=0.00$ is divided into smaller superparamagnetic clusters for $x=0.02$, so that $\sigma(T)$ becomes temperature dependent.

A split of the zero-field-cooled and field-cooled data (second inset of Fig. 1) was observed around 130 K for $x=0.02$. It might be a spin-glass transition or superparamagnetic blocking temperature. We suppose the latter one is correct, because a spin-glass transition does not occur at such a high temperature for similar alloys.²⁴ Such a split was not observed above 2 K for $x \geq 0.05$ indicating that these clusters become smaller with a much lower blocking temperature.

Values of χ_T vs T at 1 T and 5×10^{-4} T for $0.02 \leq x \leq 0.20$ are shown in Fig. 2. If clusters exist, χ_T at the low field (5×10^{-4} T) should be much higher than that at high field (1 T) by the σ/H term in Eq. (3.1). At low field χ_T is much larger than at high field for $x=0.02$, because the unsaturated $\sigma(T)$ are dominant at the low field. The room-temperature values are comparable because of a smaller $\sigma(T)$ at room temperature. For $x=0.05$, we did not observe either any split of zero-field-cooled and field-cooled magnetization nor a nonlinear M - H plot at $H \leq 0.1$ T at 77 K. However, the high- and low-field values of χ_T differ appreciably at low T , presumably because some ferromagnetic clusters of small magnetic moments are present. At $x=0.10$, the

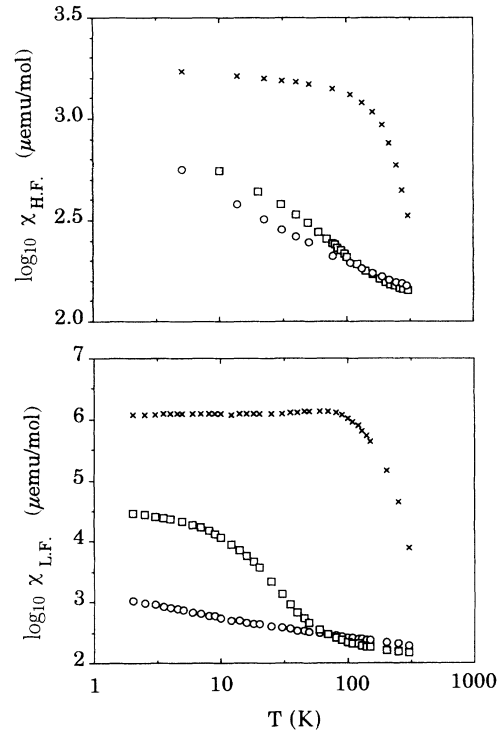


FIG. 2. Total magnetic susceptibility (M/H) measured at high field (1 T) and low field (5×10^{-4} T) in logarithmic scale. Symbols are the same as in Fig. 1. Unsaturated cluster moments dominate for $x \leq 0.05$ at the low field. Note that both susceptibilities are about the same at $x=0.10$, indicating the absence of any detectable clusters for $T \geq 10$ K.

high- and low-field values of χ_T are equal, implying the absence of any ferromagnetic clusters in the paramagnetic matrix. The impurity trace analysis indicates a few 100 ppm of Co and Fe (Table I) in all of the melt spun $\text{Ni}_{0.80-x}\text{Cr}_x\text{P}_{0.20}$ alloys made with Ni_2P and CrP powders. Such ferromagnetic impurity contents for melt spun alloys are common.²⁵ The temperature dependence of $\chi(T)$ for $x \geq 0.10$ may originate from the local moments associated with ferromagnetic trace elements.

Recently, Dobrosavljević, Kirkpatrick, and Kotliar²⁶ argued that the local Kondo-impurity density $n(T)$ is proportional to $T^{\alpha(T)}$ at low temperatures with an impurity susceptibility χ_{impurity} proportional to $1/T^{1-\alpha(T)}$. The power $\alpha(T)$ approaches 0 as T approaches 0 at temperatures in the 1 mK–1 K for a highly disordered metal, which is a non-Fermi-liquid behavior. In the temperature range 10–300 K, $\alpha(t)$ is approximately a constant, unless interactions between the impurities exist. The magnetization of $\text{Ni}_{0.80-x}\text{Cr}_x\text{P}_{0.20}$ alloys at $x=0.10$, 0.20, and 0.25 are in good agreement with this prediction. Similar behavior has been observed for $\text{Fe}_{0.33}\text{Zr}_{0.67}$ (Ref. 23) with $p=1-\alpha=0.58$. The values of p and χ_0 in a power-law fit for $\text{Ni}_{0.80-x}\text{Cr}_x\text{P}_{0.20}$ alloys are extracted only for $x=0.10$, 0.20, and 0.25. These parameters along with those from the Curie fit to χ_T are given in Table I. This power fit did not work well for $x \leq 0.05$, because of the saturation behavior of superparamagnetic clusters.

The resistivity (ρ) of $\text{Ni}_{0.80-x}\text{Cr}_x\text{P}_{0.20}$ alloys (Fig. 3)

TABLE I. The chemical content of each alloy, including trace magnetic impurities as determined from wavelength dispersion spectroscopy, and the fitting parameters of $\chi(T)$ for $x = 0.00$ and χ_T for $x > 0.00$ with Curie-Weiss fit and a power-law fit.

x	Chemical content (atomic ratio)			Magnetic element impurity		$\chi_T = \chi_0 + \frac{C}{T + \theta}$			$\chi_T = \chi_0 + \frac{C}{T^p}$		
	Ni	Cr	P	Co (ppm)	Fe (ppm)	χ_0 ($\mu\text{emu/mol}$)	C ($\mu\text{emu K/mol}$)	θ (K)	χ_0 ($\mu\text{emu/mol}$)	C ($\mu\text{emu K/mol}$)	p
0.00	0.793	0.000	0.206	460	90	63.1 ^a	39 ^a	0.2 ^a	63.1 ^a	37.2 ^a	1.003 ^a
0.02	0.780	0.018	0.201	630	633	b			b		
0.05	0.751	0.05	0.198	660	200	88.6	15539	23.5	b		
0.10	0.700	0.099	0.200	490	210	137.8	5862	9.0	72.9	1017.2	0.454
0.20	0.614	0.191	0.194	300	350	166.9	6047	17.6	115.4	704.2	0.413
0.25	0.560	0.246	0.194	390	340	148.2	3537	13.0	95.8	456.3	0.359

^a $\chi(T) = \delta M / \delta H$ at high field is fitted for $x = 0.00$, and $\chi_T = M / H$ is otherwise.

^b $\chi_T = M / H$ cannot be fitted because of large amount of clusters. See Fig. 2.

increases with ETM (Cr) content, as is commonly observed in ETM-LTM binary alloys. Mooij²⁷ showed that this resistivity is related with the sign of the temperature coefficient of resistivity (TCR). TCR for metallic amorphous alloys changes sign at a resistivity of approximately $150 \mu\Omega \text{ cm}$. The inset shows this general rule is also true for $\text{Ni}_{0.80-x}\text{Cr}_x\text{P}_{0.20}$ alloys.

The Ni-P alloys which have small resistivities relative to the critical value of $150 \mu\Omega \text{ cm}$ have been treated as a free electron like alloys that can be reasonably well described by the Faber-Ziman theory,^{19,25,28} where the static structure factor $S(2k_F)$ determines the sign of TCR. The resistivity minimum for $x = 0.00$ (Fig. 4) has been generally considered as resulting from the Kondo effect due to the magnetic impurities.^{19,29} We suppose however the quantum interference effects among the conduction electrons are responsible for the sign change of TCR with Cr content in Fig. 3, because high resistivity, $\rho \geq 150 \mu\Omega \text{ cm}$, is a good indication for multiple scattering and interference. Howson³⁰ argued that the negative TCR is actually related to the quantum-mechanical correction due to the multiple scattering of electrons with short elastic mean free paths, which leads to weak localization. In

weak localization, in the presence of spin-orbit scattering the anomalous resistivity can be written as³¹

$$\rho_{\text{WL}}(T) = \rho^2 A (\sqrt{t} - 3\sqrt{t+1}),$$

$$\text{where } A = \frac{e^2}{2\pi^2 \hbar \sqrt{D\tau_{\text{SO}}}}, \quad t = \frac{\tau_{\text{SO}}}{4\tau_{\text{ie}}}, \quad (3.2)$$

τ_{ie} , τ_{SO} are electron dephasing times due to inelastic scattering and spin-orbit scattering, respectively, and the parameter D is the electronic diffusion coefficient. The temperature dependence of ρ_{WL} originates mainly from that of $\tau_{\text{ie}} = \alpha T^{-n}$ ($2 < n < 4$), due to the electron phonon scattering. ρ_{WL} has a maximum at $t = \frac{1}{8}$, thus the slope $\partial\rho/\partial T$ is negative for $t > \frac{1}{8}$. This general argument for negative TCR is actually observed in the temperature dependence of resistivity (Fig. 4). In accordance with this argument, the magnetoresistance of $\text{Ni}_{0.80-x}\text{Cr}_x\text{P}_{0.20}$ alloys at 4 K (Fig. 5) shows an increase of weak localization effects with the Cr content. The positive magnetoresistance in Fig. 5 is characteristic of weak localization in the presence of appreciable spin-orbit scattering.

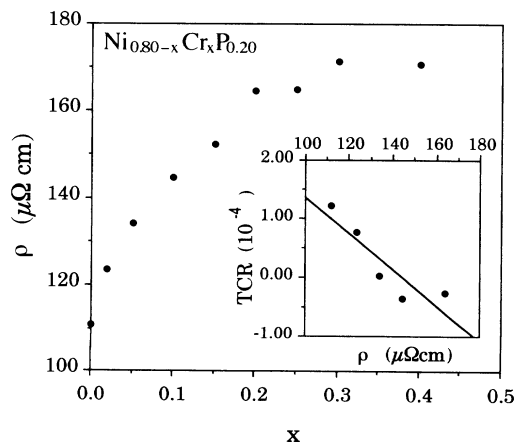


FIG. 3. The resistivity vs x of $\text{Ni}_{0.80-x}\text{Cr}_x\text{P}_{0.20}$ alloys. Inset is a Mooij diagram which shows the change of sign of TCR with high resistivity.

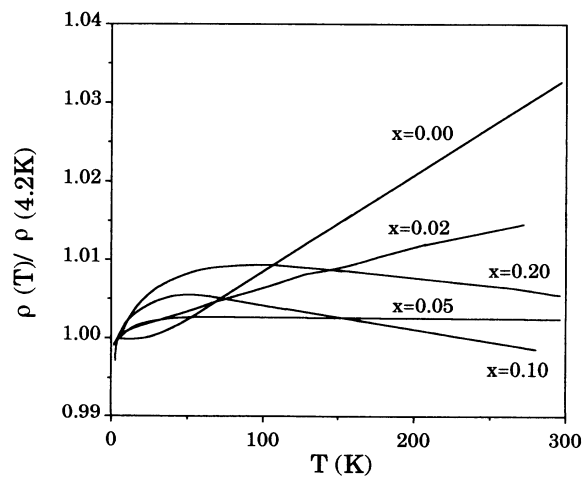


FIG. 4. Temperature dependence of resistivity of $\text{Ni}_{0.80-x}\text{Cr}_x\text{P}_{0.20}$ alloys. Note that $\rho(T)$ for $x = 0.00$ exhibits a minimum, flattens for $x = 0.05$, and then shows a maximum for $x = 0.10$ and 0.20 .

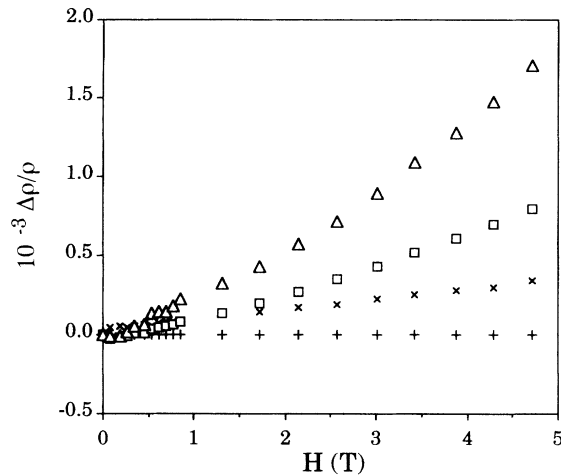


FIG. 5. Magnetoresistance of $\text{Ni}_{0.80-x}\text{Cr}_x\text{P}_{0.20}$ alloys at 4 K. Note that the strength of weak localization effects increases with Cr content.

The weak localization effect for smaller Cr content is weaker, not only because the resistivity is smaller, but also because the higher content of magnetic impurities for the low Cr concentrations (as evidenced by the saturation moments in the inset of Fig. 1) reduces constructive coherence of electron wave functions by magnetic scattering.

The temperature dependence of R_H for several compositions is shown in Fig. 6. The increase of R_H as T decreases for $x \geq 0.05$ is similar to that of the magnetic susceptibility of these alloys. R_H for $x = 0.00$ is almost temperature independent as is the high-field susceptibility. R_H changes sign near 20 K for the $x = 0.20$ sample. Such a sign change of the Hall coefficient of a paramagnetic amorphous alloy with temperature has not been reported to our knowledge. It provides convincing proof that the positive values of R_H in this alloy system result from an extraordinary contribution to the Hall coefficient that is positive.

There appears to be an additional linear term in the temperature dependence of R_H for these alloys that is not present in χ_T . Consequently, we have fitted the temperature dependence of R_H for $x = 0.05, 0.10$, and 0.20 to

$$R_H = R_H^0 - bT + D \left[\frac{C}{T + \theta} + \chi_0 - \chi_d \right], \quad (3.3)$$

where the last contribution clearly represents the positive

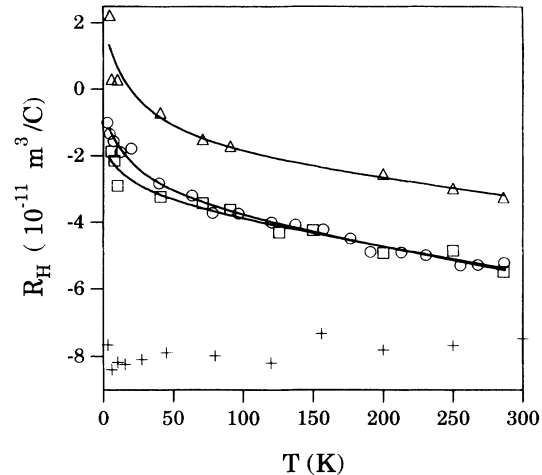


FIG. 6. The temperature dependence of R_H for $\text{Ni}_{0.80-x}\text{Cr}_x\text{P}_{0.20}$ alloys. Note the sign change of R_H at $x = 0.20$ at low temperature. The data are fitted to $R_H = R_H^0 - bT + D[C/(T + \theta) + \chi_0 - \chi_d]$ where C , χ_0 , and θ are taken from Table I. Values of R_H^0 , b , and D are given in Table II. Symbols are the same as in Fig. 1.

extraordinary term in the Hall coefficient that is responsible for the change of sign of R_H for the $x = 0.20$ sample as a function of temperature. (χ_d is the diamagnetic contribution to the susceptibility. We have chosen the Curie-Weiss description for χ_T because the power law did not describe the results well for $x = 0.05$, but the power-law description could have been easily used without changing any conclusions.) Values of these parameters are given in Table II.

The large $-bT$ contribution to R_H in this system is quite puzzling. Schulte *et al.*³² have reported a small variation in R_H for Zr and Ti alloys which appeared to be linear in temperatures for $T > 100$ K. At low temperatures this variation is proportional to \sqrt{T} and has been identified³³ with electron interaction effects. According to Altshuler and Arnov,³⁴ the magnitude of these effects for R_H should be proportional to their contribution to resistivity,

$$\frac{\Delta R_H}{R_H} = \frac{2\Delta\rho(T)}{\rho(0)}. \quad (3.4)$$

As shown in Fig. 4, electron interference effects are much too small to account for this large $-bT$ contribution to R_H .

TABLE II. Parameters for $R_H(T) = R_H^0 - bT + D[C/(T + \theta) + \chi_0 - \chi_d]$ and the ratio of the effective spin-orbit parameter to the free-electron value $\lambda_{\text{SO}}^{\text{SJ}}/\lambda_{\text{SO}}^{\text{free}}$. Parameters C , θ , and χ_0 are taken from Table I. The term $D[C/(T + \theta) + \chi_0 - \chi_d]$ is identified as the side-jump contribution $R_H^{\text{SJ}}\chi_v$ to the Hall coefficient.

x	R_H^0 ($10^{-11} \text{ m}^3/\text{C}$)	b ($10^{-14} \text{ m}^3/\text{C K}$)	bT (300 K) ($10^{-11} \text{ m}^3/\text{C}$)	D ($10^{-14} \text{ m}^3/\text{mol/C} \mu\text{emu}$)	$R_H^{\text{SJ}}\chi_v$ (300 K) ($10^{-11} \text{ m}^3/\text{C}$)	$\lambda_{\text{SO}}^{\text{SJ}}/\lambda_{\text{SO}}^{\text{free}}$
0.05	-3.80	7.0	2.1	2.6	0.3	400
0.10	-4.07	7.2	2.2	4.3	0.6	665
0.20	-2.85	4.7	1.4	6.2	1.0	1024

The extraordinary term is $D[C/(T+\theta)+\chi_0-\chi_d]$ in this fit. A logical source for this anomalous or extraordinary contribution to R_H is the side-jump mechanism described in Eqs. (1.1)–(1.4). From the parameters in Table I, it is clear that the temperature dependent part $C/(T+\theta)$ contributes only a part of χ_v . This is a significant difference between the $\text{Ni}_{0.80-x}\text{Cr}_x\text{P}_{0.20}$ alloys and Zr-Fe (Ref. 8) systems where the temperature-dependent part of the susceptibility for Zr-Fe dominates the total susceptibility. The relative values of the different contributions (the Lorentz contribution R_H^0 , the unexpected linear contribution $-bT$, and the side-jump contribution $R_H^{\text{SJ}}\chi_v$) at room temperature are tabulated for $x=0.05, 0.10$, and 0.20 . The values of the ratio of $\lambda_{\text{SO}}^{\text{SJ}}$ determined from Eq. (1.2) to the free-electron value $\lambda_{\text{SO}}^{\text{free}}$ are also given for these compositions in Table II. These are much smaller than values estimated for 3-*d* and 4-*d* alloys with significantly larger early transition-metal compositions.^{10,12} As expected from Eq. (1.4), $\lambda_{\text{SO}}^{\text{SJ}}$ increases as the Cr concentration increases.

As shown in Fig. 7, the room-temperature values of R_H for these alloys increase with increasing Cr content. The sign changes from negative to positive near values of $x=0.25$. We argue that this change is also related to the extraordinary contribution to R_H , i.e., the increase in $\lambda_{\text{SO}}^{\text{SJ}}$ as the location of the Fermi level is pushed from the Ni *d* band further into the Cr *d* band with Cr concentration produces the increase in R_H and results in positive values over the entire temperature range above $x=0.25$. It is very fortunate in demonstrating that the source of the positive Hall coefficient in this alloy system is due to an extraordinary contribution and in identifying that extraordinary contribution that $C/(T+\theta)$ and $\lambda_{\text{SO}}^{\text{SJ}}$ were sufficiently large to produce the change in sign of R_H with temperature for the $x=0.20$ alloy. We argue that such an extraordinary contribution is responsible for the positive values of R_H observed in many similar amorphous alloys containing early transition-metal elements.

In Fig. 8, the extraordinary contribution $R_H^{\text{SJ}}\chi_v = R_H - (R_H^0 - bT)$, is plotted against $\chi_v\rho^2$ to illus-

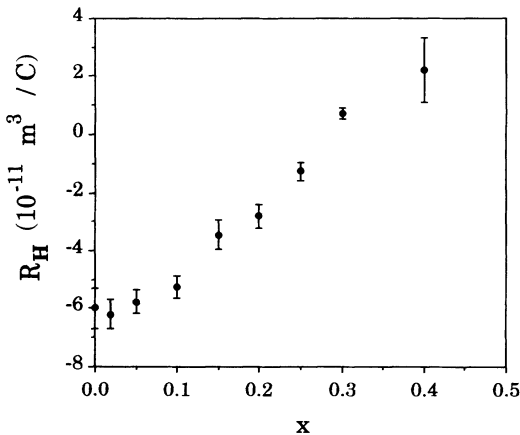


FIG. 7. R_H vs x for $\text{Ni}_{0.80-x}\text{Cr}_x\text{P}_{0.20}$ alloys. R_H increases with x , as expected from the side-jump effect, because the location of the Fermi level moves from the upper half of the Ni band to the lower half of the Cr band.

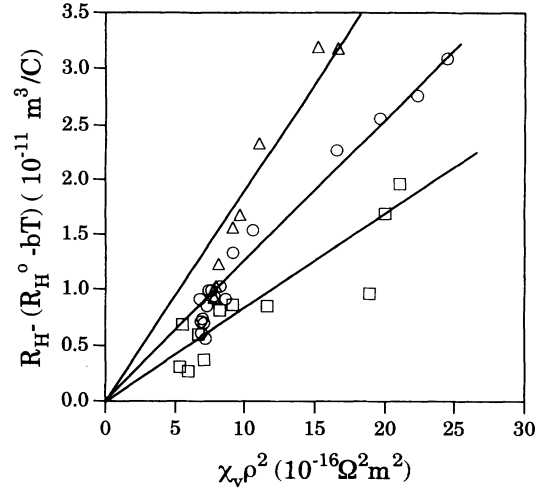


FIG. 8. The extraordinary part of Hall coefficients [$R_H^{\text{SJ}}\chi_v = R_H - (R_H^0 - bT)$] vs $\chi_v\rho^2$ for $\text{Ni}_{0.80-x}\text{Cr}_x\text{P}_{0.20}$ alloys. Note that the χ_v in the x axis is transformed to unitless volume susceptibility, to compare with Eq. (1.2). Symbols are the same as in Fig. 1.

trate the agreement with the identification of the extraordinary term with one having the attributes of the side-jump contribution as described in Eq. (1.2). Although the resistivity for these alloys shows an appreciable change with composition (Fig. 3), the ρ^2 dependence of R_H is more clearly demonstrated by measurements on Ti-Al alloys³⁵ and Ti-Ni, Zr-Ni, and Hf-Ni alloys³⁶ previously studied. When considered as a body of work, these experiments provide a convincing case that an extraordinary contribution to R_H which is proportional to ρ^2 and χ_v is responsible for the positive values of the Hall coefficient observed in amorphous metal alloys containing early transition-metal components. The side-jump mechanism provides a qualitative explanation of the compositional variation of the magnitude and sign.^{12,15}

IV. SUMMARY AND CONCLUSIONS

The temperature dependence of resistivity and magnetoresistance measurements show that the resistivity of $\text{Ni}_{0.80-x}\text{Cr}_x\text{P}_{0.20}$ alloys changes with x from the Ziman-Faber type to that dominated by quantum interference with appreciable spin-orbit scattering. We have observed a sign change of R_H with temperature for a paramagnetic amorphous $\text{Ni}_{0.80-x}\text{Cr}_x\text{P}_{0.20}$ alloy for $x=0.20$ which demonstrates that a positive extraordinary contribution to R_H is responsible for both the temperature and composition dependence of R_H in this system. The sign change with temperature which results from the additive, positive extraordinary contribution in this system provides an important difference from the measurements on Zr-Fe,⁸ where R_H is proportional to χ_T but always positive. For the $\text{Ni}_{0.80-x}\text{Cr}_2\text{P}_{0.20}$ alloys it is thus not possible to argue that the ordinary Hall coefficient is proportional to the susceptibility, but that its sign is determined by some other effect, as has been done for the Zr-Fe data.³⁷ This side-jump mechanism describes this extraordinary contribution well. We note that Movaghar and

Cochrane^{37,38} have raised objections to the derivation of the side-jump contribution. Nevertheless in their calculations, they did find a term that reduces to Eq. (1.3) without having to introduce the idea of a side jump as originally proposed by Berger. We have used the original term "side-jump" to describe the anomalous term without regard to the controversy regarding its actual origin. A significant contribution to R_H which is linear in T whose origin is not understood was also observed. A gradual change of magnetism from a large-cluster-dominant phase to a Kondo-impurity-like phase as x increases has been observed also. In contrast to conventional Curie-Weiss behavior, the susceptibility can be equally well described by a power law, $\chi_T = C/T^p + \chi_0$, with $p = 0.45, 0.41$, and 0.36 for $x = 0.10, 0.20$, and 0.25 ,

respectively, throughout the temperature region 10–300 K. Such behavior is consistent with that predicted²⁶ for a Kondo-impurity phase.

ACKNOWLEDGMENTS

The work at Texas A&M University was supported in part by the Robert A. Welch Foundation (Houston, TX) Grant No. A-0514, the Texas Advanced Technology Program (3606), and by NSF (Grant No. DMR-89-03135), while that at the University of Texas was supported by the Robert A. Welch Foundation (F-1191) and NSF (Grant Nos. DMR 91-04194 and DMR 91-58089). The authors would like to thank Dr. K. D. D. Rathnayaka for helpful technical support and concern.

¹D. G. Naugle J. Phys. Chem. Solids **45**, 367 (1984).

²U. Mizutani, Prog. Mater. Sci. **28**, 97 (1983).

³P. C. Colter, D. G. Naugle, T. W. Adair, and W. L. Johnson, J. Phys. (Paris) Colloq. **39**, C6-955 (1978).

⁴P. C. Colter, T. W. Adair, and D. G. Naugle, Phys. Rev. B **20**, 2959 (1979).

⁵G. F. Weir, W. A. Howson, B. L. Gallagher, and G. J. Morgan, Philos. Mag. **47**, 163 (1983).

⁶M. A. Howson and G. J. Morgan, Philos. Mag. **51**, 439 (1985).

⁷D. Nguyen-Manh, D. Mayou, G. T. Morgan, and A. Pasturel, J. Phys. F **17**, 999 (1987).

⁸M. Trudeau, R. W. Cochrane, D. V. Baxter, J. O. Ström-Olsen, and W. B. Muir, Phys. Rev. B **37**, 4499 (1988).

⁹L. Berger, Phys. Rev. B **32**, 4559 (1970).

¹⁰L. Berger and G. Bergmann, in *The Hall Effect and its Applications*, edited by C. L. Chien and C. R. Westgate (Plenum, New York, 1980), p. 55.

¹¹T. R. MacGuire, R. J. Gambino, and R. C. O'Handley, in *The Hall Effect and its Applications* (Ref. 10), p. 137.

¹²K. Rhie, D. G. Naugle, B.-h. O, and J. T. Markert, Phys. Rev. B **48**, 5973 (1993).

¹³K. Rhie, D. G. Naugle, and A. K. Bhatnagar, Z. Phys. B **78**, 411 (1990).

¹⁴K. Rhie and D. G. Naugle, Phys. Lett. A **149**, 301 (1990).

¹⁵K. Rhie and D. G. Naugle, in *Ordering Disorder: Prospect and Retrospect in Condensed Matter Physics*, edited by V. Srivastava, A. K. Bhatnagar, and D. G. Naugle, AIP Conf. Proc. No. 286 (AIP, New York, 1993), p. 61.

¹⁶P. Oelhafen, in *Glassy Metals II*, edited by H. Beck and H.-J. Güntherodt (Springer-Verlag, New York, 1983), p. 283.

¹⁷W. L. Johnson and M. Tenhover, in *Glassy Metals: Magnetic, Chemical and Structural Properties*, edited by R. Hasegawa (CRC, Boca Raton, 1983), p. 65.

¹⁸I. Bakonyi, J. Magn. Magn. Mater. **50**, 111 (1985).

¹⁹A. Berrada, M. Lapierre, B. Loegel, P. Panissod, and C. Robert, J. Phys. F **8**, 845 (1978).

²⁰W. A. Heines, C. U. Mozelewski, R. N. Paolino, and R. Hasegawa, Solid State Commun. **39**, 669 (1981).

²¹A. Bugstaller, W. Socher, J. Voithländer, I. Bakonyi, E. Tóth-Kaadár, A. Lovas, and H. Ebert, J. Magn. Magn. Mater. **109**, 117 (1992).

²²R. W. Cochrane and M. Trudeau, J. Appl. Phys. **57**, 3207 (1985).

²³K. Rhie, D. G. Naugle, B.-h. O, J. T. Markert, A. Morrish, and X. Z. Zhou (unpublished).

²⁴J. Durand, in *Glassy Metals: Magnetic, Chemical and Structural Properties* (Ref. 17), p. 109.

²⁵J. P. Carini, S. R. Nagel, L. K. Varga, and T. Schmit, Phys. Rev. B **27**, 7589 (1983).

²⁶V. Dobrosavljević, T. R. Kirkpatrick, and G. Kotliar, Phys. Rev. Lett. **69**, 1113 (1992).

²⁷J. H. Mooij, Phys. Status Solidi A **17**, 321 (1973).

²⁸P. J. Cote, Solid State Commun. **18**, 1311 (1976).

²⁹Y. S. Tyan and L. E. Toth, J. Elec. Mater. **3**, 791 (1974).

³⁰M. A. Howson, J. Phys. F **14**, L25 (1984).

³¹H. Kukuyama and K. Hoshino, J. Phys. Soc. Jpn. **50**, 2131 (1981).

³²A. Schulte, A. Ekert, G. Fritsch, and E. Lüscher, J. Phys. F **14**, 1877 (1984).

³³B. L. Gallagher, D. Greig, and M. A. Howson, J. Phys. F **14**, L225 (1984).

³⁴B. L. Altshuler and A. G. Arnov, in *Electron-Electron Interaction in Disordered Systems, Modern Problems in Condensed Matter Sciences*, edited by A. L. Efros and M. Polak (North-Holland, Amsterdam, 1985), Vol. 10.

³⁵K. D. D. Rathnayaka, B. D. Hennings, and D. G. Naugle, Phys. Rev. B **48**, 6937 (1993).

³⁶K. D. D. Rathnayaka, K. Rhie, B. D. Hennings, and D. G. Naugle, J. Phys.: Condens. Matter **5**, 7251 (1993).

³⁷B. Movaghar and R. W. Cochrane, Phys. Status Solidi B **116**, 311 (1991).

³⁸B. Movaghar and R. W. Cochrane, Z. Phys B **32**, 217 (1992).